Research on the strain gauge mounting scheme of track wheel force measurement system based on high-speed wheel/rail relationship test rig

Received 12 May 2024
Revised 5 June 2024
Accepted 11 June 2024

Yuanwu Cai, Bo Chen and Chongyi Chang
Railway Science and Technology Research and Development Center, China Academy of Railway Sciences Corporation Limited, Beijing, China

Abstract

Purpose – This paper aims to analyze the stress and strain distribution on the track wheel web surface and study the optimal strain gauge location for force measurement system of the track wheel.

Design/methodology/approach – Finite element method was employed to analyze the stress and strain distribution on the track wheel web surface under varying wheel-rail forces. Locations with minimal coupling interference between vertical and lateral forces were identified as suitable for strain gauge installation.

Findings – The results show that due to the track wheel web's unique curved shape and wheel-rail force loading mechanism, both tensile and compressive states exit on the surface of the web. When vertical force is applied, Mises stress and strain are relatively high near the inner radius of 710 mm and the outer radius of 1110 mm of the web. Under lateral force, high Mises stress and strain are observed near the radius of 670 mm on the inner and outer sides of the web. As the wheel-rail force application point shifts laterally toward the outer side, the Mises stress and strain near the inner radius of 710 mm of the web gradually decrease under vertical force while gradually increasing near the outer radius of 1110 mm of the web. Under lateral force, the Mises stress and strain on the surface of the web remain relatively unchanged regardless of the wheel-rail force application point. Based on the analysis of stress and strain on the surface of the web under different wheel-rail forces, the inner radius of 870 mm is recommended as the optimal mounting location of strain gauges for measuring vertical force, while the inner radius of 1143 mm is suitable for measuring lateral force.

Originality/value – The research findings provide valuable insights for determining optimal strain gauge locations and designing an effective track wheel force measurement system.

Keywords Track wheel, High-speed wheel/rail relationship test rig, Instrumented wheelset, Strain gauge, Finite element

Paper type Research paper

1. Introduction

Wheel-rail contact forces are important items in infrastructure testing and are an important basis for evaluating the smoothness and safety of vehicle operation. Therefore, obtaining wheel-rail contact forces accurately has important theoretical and practical significance. Instrumented wheelsets can continuously and in real-time measure wheel-rail contact forces, thereby analyzing the quality of train operation and line status and providing important

Funding: The study was funded by the Fund Project of China Academy of Railway Sciences Corporation Limited [Grant No. 2022YJ194, 2023YJ254].

Railway Sciences
Vol. 3 No. 4, 2024
pp. 503-513
Emerald Publishing Limited
e-ISSN: 2755-0915
p-ISSN: 2755-0907
DOI 10.1108/RS-05-2024-0015

technical means for railway safety assessment (Hou, Wang, & Zeng, 2010; Bracciali, Cavaliere, & Macherelli, 2014). The instrumented wheelset directly perceives the wheel-rail contact forces by attaching strain gauges to the surface of the wheel web, using the wheelset itself as a sensor. The strain gauge undergoes deformation with the deformation of the wheel web. When the metal foil inside the strain gauge is subjected to tension or compression, its own resistance value will change. By collecting the resistance change value of the strain gauge and calculating it, relevant data on the surface deformation of the wheel web can be obtained, and then the corresponding wheel-rail contact forces can be obtained (Ren, 2012). The wheel-rail contact forces are computed while the train is running based on the signals received from strain gauge bridges. These signals are influenced by various factors including the lateral force, vertical force, contact point and rotational angle.

There are mainly two approaches for continuous wheel-rail contact force measurement. One is the classic method, which involves solving equations derived from strain gauge signals and accounting for the combined effects of vertical and lateral forces. The other method individually measures vertical and lateral forces using dedicated vertical and lateral bridges. The classic approach employs strain gauges mounted to a wheel web to generate distinctive waveforms, such as sinusoidal and triangular waves. These waveforms are electronically integrated to produce continuous signals that are directly proportional to the lateral and vertical forces. These forces are subsequently determined by solving corresponding equations derived from the strain gauge signals. Numerous studies have focused on analyzing harmonic characteristics under various bridging schemes and refining the calculation processes accordingly. However, these strategies may not be universally applicable, such as certain wheelsets with curved webs. In contrast to the classic approach, an alternative method is to mitigate undesired coupling interference between vertical and lateral forces through the selection of strain gauge placements. Vertical and lateral forces are separately measured using distinct vertical and lateral bridges. Vertical bridges are engineered to exclusively detect vertical wheel-rail contact forces, while lateral bridges are sensitive solely to lateral wheel-rail contact forces. The primary drawback of these methods lies in the challenge of selecting optimal strain gauge locations to establish a strain bridge that is exclusively sensitive to either vertical or lateral forces.

Instrumented wheelsets generally require the placement of strain gauges at specific radius locations, such as in areas with less coupling interference between lateral and vertical forces, in order to obtain good waveforms and improve detection accuracy. For high-speed railway wheels (Li, 2015; Zhu, 2015; Otter, El-Sibaie, & Higgins, 1991) and subway wheels (Zhong, Kou, Zhang, & Wang, 2020; Cai *et al.*, 2023; Hao, 2023), many research studies have been conducted on the placement of strain gauges in instrumented wheelsets. Zeng *et al.* (1998) established an analysis method by using a harmonic analyzer; the measuring bridge design was summed up with the digital filter design and gave a theory of high accuracy load measuring wheelsets. Chang, Wang, Li, and Zeng (2007) presented a numerical method based on the finite element method to simulate strain in the wheel disc in the vertical and horizontal wheel/rail loads, studied the relation between the strain in the wheel and the point where the vertical and horizontal wheel/rail load acts and found the best locations of sticking strain gauges. Chu, Li, and Zu (2011) used finite element analysis to analyze the wheel stress map of static loads for high-speed Electric Multiple Unit (EMU), designed strain gauge bridges for the instrumented wheelset based on the Finite Element Analysis (FEA) results and evaluated errors induced by centrifugal force and dynamic response, which is helpful for design and application of the instrumented wheelset. Ren and Chen (2019) proposed a method based on state space theory and calculated the wheel-rail contact force by the recurrence relation and the signals from strain gauge bridges on wheel web. The effectiveness and accuracy of this new method was demonstrated and discussed by estimation results with the numerical simulations and also applied to two field tests, including one was conducted in a loop test line

using a high-speed train, and the other in an urban line with a light rail vehicle. However, these research studies often target at specific high-speed railway or subway wheel models and do not have universality.

Contemporary instrumented wheelsets are constructed upon standard wheelsets with monoblock wheels and incorporate strain gauges for sensing purposes. There are notable distinctions in the location and arrangement of strain gauges in the instrumented wheelsets. Strain gauges are strategically located on both the inner and outer sides of the wheel at precise radial distances from the center. Determining the most suitable radial distances typically involves conducting finite element analyses of wheel strains, which is a primary challenge in the development of instrumented wheelsets. At present, there is no reasonable standard to determine the radius location of a strain gauge. In practical operation, for specific wheel objects, it is necessary to analyze them specifically in order to determine the placement location of strain gauges and design a precise force measurement system (Bižić, Petrović, Tomić, & Djinović, 2017; Cazzulani *et al.*, 2017). Moreover, challenges arise concerning the identification of the optimal layout, quantity and method of connecting strain gauges, as well as resolving calibration procedures, managing signal transmission and other associated tasks. The fundamental objective throughout the resolution of these complexities is to attain the utmost precision in measurement accuracy.

During vehicle operation, the contact point between wheel and rail is constantly changing, especially when passing through curves, turnouts and hunting motions, where the contact point is far away from the rolling circle (Guo, 2020). The existing research on instrumented wheelset, often assumes that the contact point is on a rolling circle without considering the position change of the contact point, which may cause errors in data measurement results and calibration experiments (Hu, Zu, Zhang, Chu, & Zhang, 2012; Zhang, 2016). With the rapid development of high-speed railways and the significant improvement of locomotive and vehicle manufacturing technology, higher requirements have been put forward for the performance of instrumented wheelsets. Developing a more scientific and advanced instrumented wheelset to reduce the impact of changes in the position of the contact point on the measurement results has become more urgent.

This paper takes the track wheel of the high-speed wheel/rail relationship test rig as the research object, whose web plate has a special curved shape, thus needs to analyze the stress and strain distribution on the surface of the track wheel web through the finite element method and studies the strain gauge placement suitable for the force measurement system of the track wheel web to meet the needs of continuous and high-precision measurement of wheel-rail contact forces. The track wheel force measurement system can be regarded as a special instrumented wheelset used to measure the wheel-rail contact forces between the test wheelset and the track wheel. The track wheel of the high-speed wheel/rail relationship test rig has special dimensions and structures, with a diameter of 3 m and a web thickness of 48–98 mm, which is very different from ordinary wheelsets. The existing research results on instrumented wheelsets cannot be directly applied and need to be studied, specifically based on the structure of the track wheel.

2. Finite element model of track wheel based on high-speed wheel/rail relationship test rig

The track wheel is a wheelset composed of two wheels with a diameter of 3 m, as shown in Plate 1. Figure 1 shows the finite element model of the track wheel built in ABAQUS software. Due to symmetry, only one side of the track wheel is used for finite element analysis. To simplify the calculation, assume the wheel axle is rigid and coupling constraints are established between the center point of the track wheel and the inner surface to simulate the connection relationship between the wheel axle and the inner surface. The track wheel model uses elastic material, with an elastic modulus of 210 GPa and a Poisson's ratio of 0.3. C3D8R hexahedral solid elements are used to divide the mesh, with a total of 300,600 elements and 343,801 nodes.

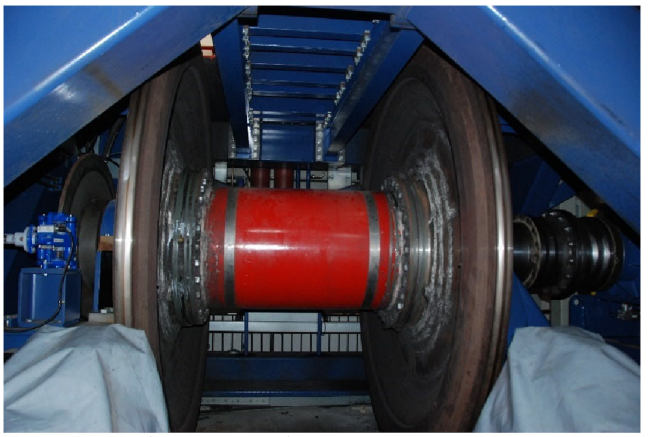

Plate 1.
The track wheel

Source(s): Authors' own work

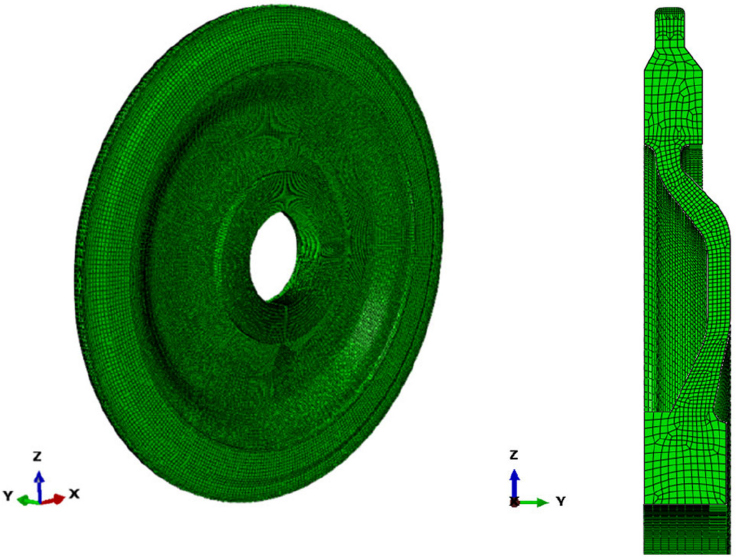

3D model of track wheel
(a)

Cross section of track wheel
(b)

Figure 1.
Finite element model of track wheel

Source(s): Authors' own work

Fixed constraints are applied to the center point of the track wheel; wheel-rail forces are applied at the wheel-rail contact point, and the stress and strain of the track wheel web under the action of wheel-rail forces are obtained through static calculation, providing a basis for selecting appropriate strain gauge locations and designing force measurement systems. When conducting finite element analysis, the wheel-rail forces are divided into vertical force and lateral force, which are applied separately, and the loading position is located at the center of the rail head. In order to analyze the influence of the position of the wheel-rail force

loading point, the deviation of the loading position from the center of the rail head by 20 mm is also calculated. The track wheel web has a special curved shape, and its cross-sectional node coordinates are shown in Figure 2, with a radius range of 536–1,166 mm.

Due to the fact that the strain gauges are attached radially to the surface of the web, the strains at the nodes on the surface of the web calculated by the finite element model need to be transformed into a strain component that is tangential to the surface and along the radial direction of the track wheel. Assuming that the strain calculated by the finite element method is in the global Cartesian coordinate system, the strain components at the nodes are ε_x, ε_y, ε_z, γ_{xy}, γ_{xz} and γ_{yz}, and in the local coordinate system, the strain components at the same node are $\varepsilon_{x'}$, $\varepsilon_{y'}$, $\varepsilon_{z'}$, $\gamma_{x'y'}$, $\gamma_{x'z'}$ and $\gamma_{y'z'}$. If there is a relationship between the global coordinate system and the local coordinate system as follows:

$$\begin{Bmatrix} x' \\ y' \\ z' \end{Bmatrix} = \begin{bmatrix} l_1 & m_1 & n_1 \\ l_2 & m_2 & n_2 \\ l_3 & m_3 & n_3 \end{bmatrix} \begin{Bmatrix} x \\ y \\ z \end{Bmatrix} \tag{1}$$

where $l_i, m_i, n_i (i = 1, 2, 3)$ are the directional cosines of the local coordinate axis relative to the global coordinate axis. The strain in the direction of the strain gauges after conversion is as follows:

$$\varepsilon_{x'} = \varepsilon_x l_1^2 + \varepsilon_y m_1^2 + \varepsilon_z n_1^2 + \gamma_{xy} l_1 m_1 + \gamma_{xz} l_1 n_1 + \gamma_{yz} m_1 n_1 \tag{2}$$

3. Stress and strain characteristics of track wheel web surface

Taking the vertical force of 75 kN and the lateral force of 20 kN as examples, the stress and strain characteristics of the track wheel web under different wheel-rail forces are analyzed, as shown in Figures 3–5. Figure 3 shows the Mises stress contour map of the track wheel surface under the action of wheel-rail forces. From Figure 3, it can be seen that under the action of

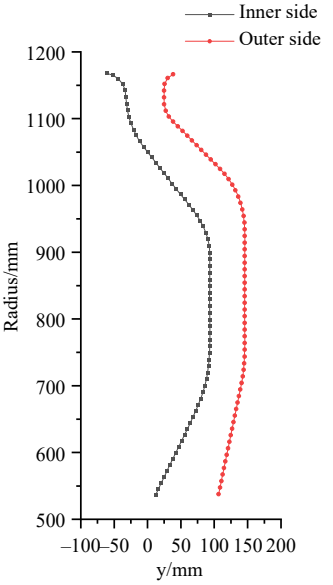

Source(s): Authors' own work

Figure 2.
Cross-sectional node coordinates of track wheel web

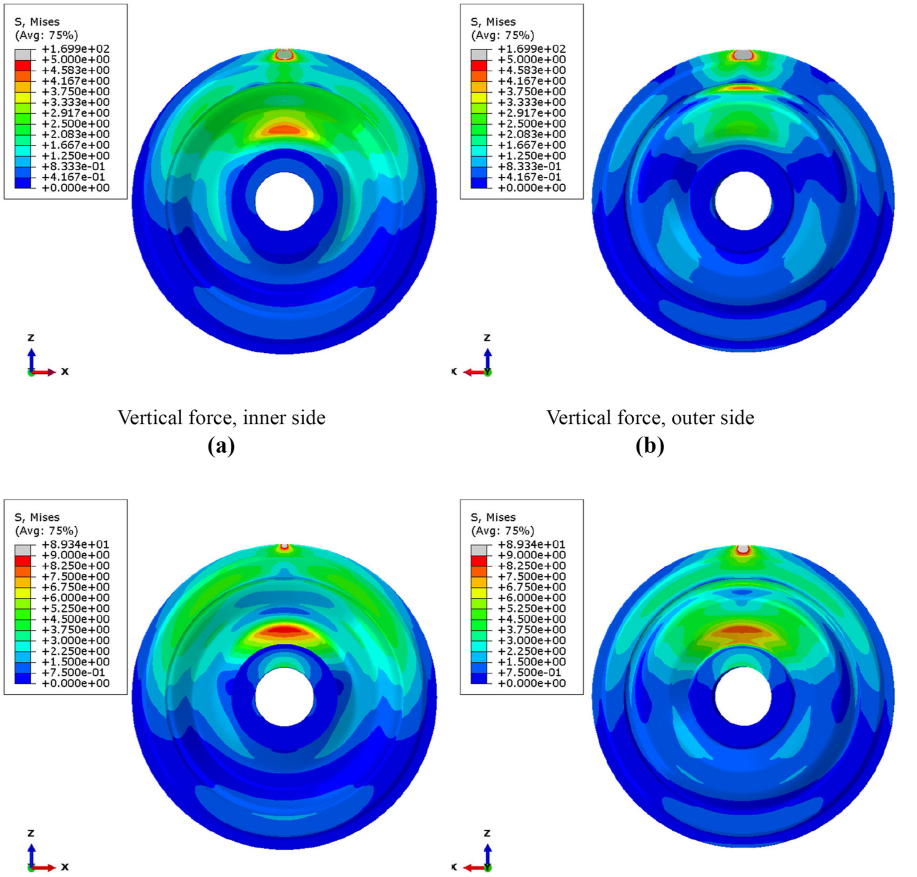

Figure 3.
Mises stress contour map of the track wheel surface

Source(s): Authors' own work

vertical force, Mises stress is relatively high near the inner radius of 710 mm and the outer radius of 1110 mm, both occurring at the curve position. Under the action of lateral force, Mises stress is relatively high near the radius of 670 mm on the inner and outer sides of the web, both occurring at the curve position near the root of the web. The locations of high Mises stress are directly below action point of the wheel-rail forces.

Figure 4 shows the circumferential variation of strain on the track wheel web surface under the action of wheel-rail forces. The angle 0 rad corresponds to the position of the wheel-rail force application point, and different curves correspond to different radius positions. From Figure 4, it can be seen that the maximum strain occurs at an angle of 0 rad. As the angle moves away from 0 rad, the strain rapidly decreases, and the greater the strain at 0 rad, the more significant this change becomes. The circumferential variation of strain on the surface of the web is symmetrically distributed around 0 rad. The surface strain of the web can be positive or negative, indicating the presence of both tensile and compressive states on the surface of the web. This is determined by the special curved shape of the web and the wheel-rail forces.

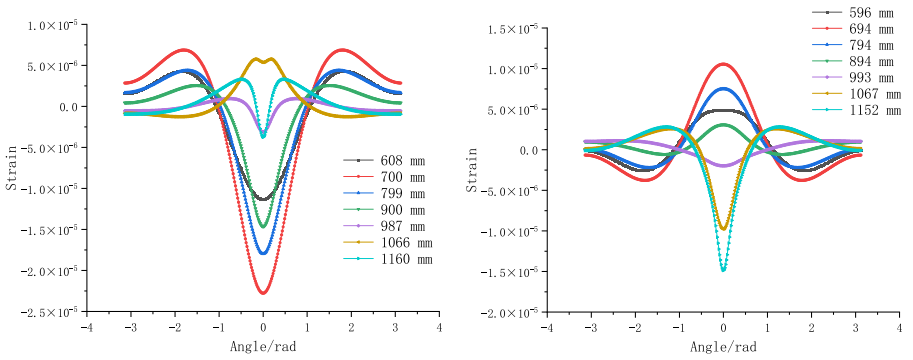

Vertical force, inner side
(a)

Vertical force, outer side
(b)

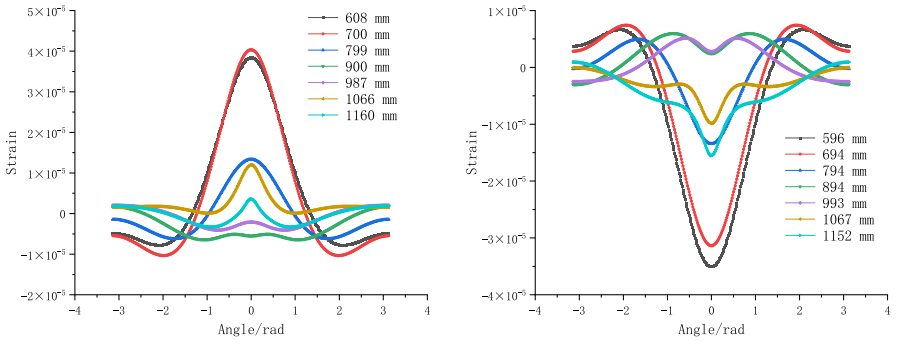

Lateral force, inner side
(c)

Lateral force, outer side
(d)

Source(s): Authors' own work

Figure 4.
Circumferential variation of strain on the track wheel web surface

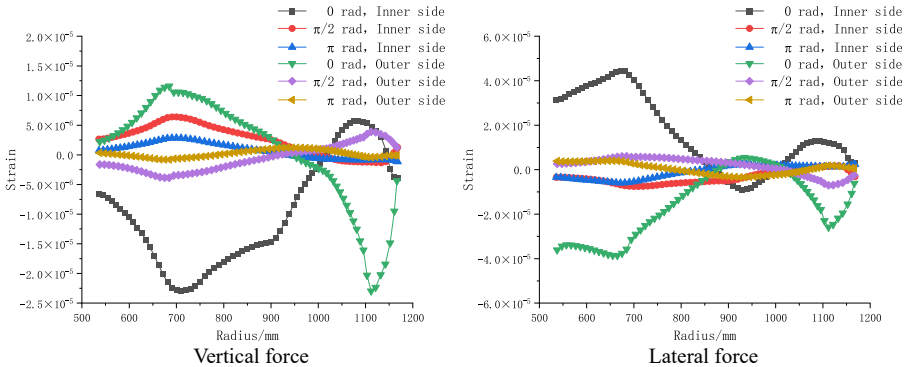

Vertical force
(a)

Lateral force
(b)

Source(s): Authors' own work

Figure 5.
Radial variation of strain on the track wheel web surface

Figure 5 shows the radial variation of strain on the track wheel web surface under the action of wheel-rail forces. The different curves correspond to the results of the inner and outer sides of the web at different angles. From Figure 5, it can be seen that the strain on the web surface is larger at an angle of 0 rad, while smaller at other angles. Under the action of vertical force, the maximum strain is near the inner radius of 710 mm and near the outer radius of 1110 mm of the web surface, both of which are compressive strains. Under lateral force, the maximum strain occurs on both the inner and outer surfaces of the web near a radius of 670 mm, with tensile strain on the inner surface and compressive strain on the outer surface. The positions of the maximum strain on the web surface under the action of wheel-rail forces are consistent with the positions of the maximum Mises stress. Positions with significant changes in strain are more sensitive to fluctuations in wheel-rail forces, which is beneficial for identifying changes in wheel-rail forces.

4. The influence of the wheel-rail force application position on the strain of the web surface

When wheel-rail forces are applied at different positions, the Mises stress contour maps of the web are shown in Figure 6, and the strains on the web surface are shown in Figure 7. The wheel-rail force application positions are laterally offset from the center of the rail head by

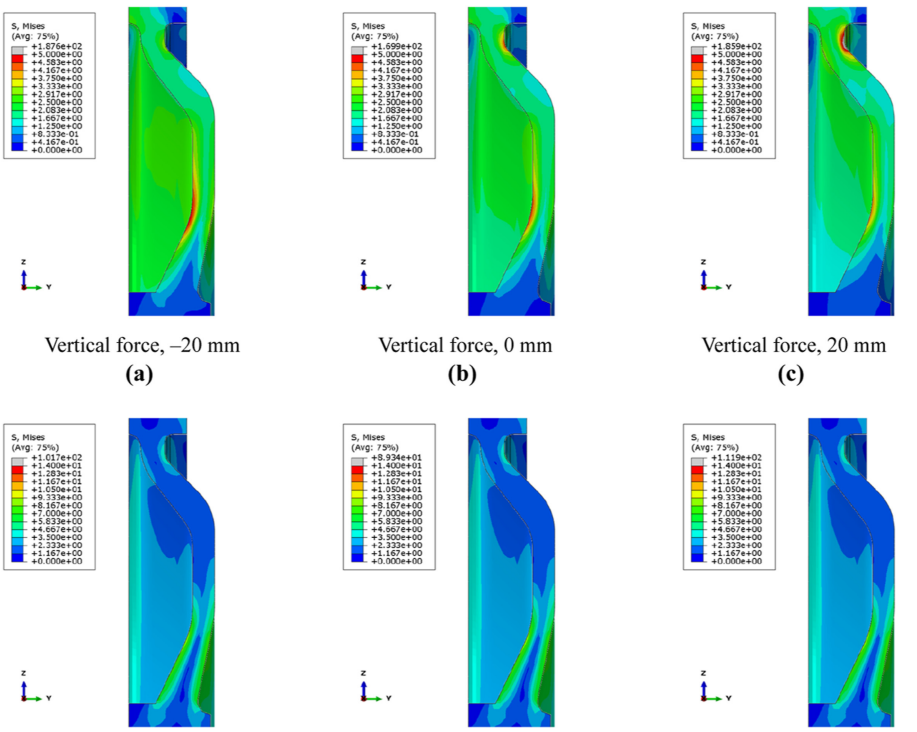

Source(s): Authors' own work

Figure 6.
Mises stress contour maps of the web cross section with different wheel-rail force application positions

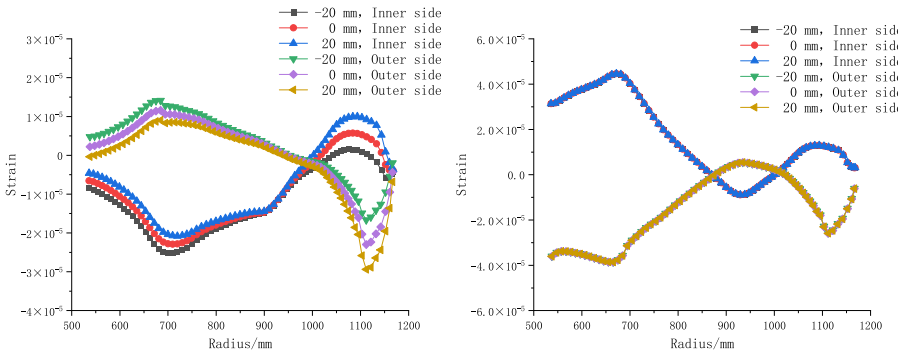

Source(s): Authors' own work

Figure 7.
Strains on the web surface with different wheel-rail force application positions

−20 mm, 0 mm and 20 mm (positive value facing outer side). From Figures 6 and 7, it can be seen that under the action of vertical force, as the wheel-rail force application position shifts laterally towards the outer side, the Mises stress and strain near the inner radius of 710 mm of the web gradually decrease, while the Mises stress and strain near the outer radius of 1110 mm of the web gradually increase. Under lateral force, the Mises stress and strain on the surface of the web do not change significantly with the wheel-rail force application position.

5. Analysis of strain gauge placement in wheel-rail force measurement system

Based on the analysis of stress and strain on the web surface under different wheel-rail forces, a selection of strain gauge mounting locations can be made, providing reference for the design of track wheel force measurement systems. The selection of mounting locations generally requires minimal coupling interference between lateral and vertical forces in order to obtain good waveforms and improve detection accuracy. Figure 8 shows the strain on the web surface under different wheel-rail forces, with a vertical force of 75 kN and a lateral force of 20 kN. For the inner side of the web, at a radius of 870 mm, the strain on the web surface is about 0 under the action of lateral force, and the strain on the web surface is relatively large under the action of vertical force, which is -1.523×10^{-5}. At the location with a radius of 1002 mm, the strain on the web surface is about 0 under lateral force and -1.554×10^{-6} under vertical force. At a radius of 1018 mm, the strain on the web surface under vertical force is about 0 and the strain on the web surface under lateral force is 3.076×10^{-6}. At the location with a radius of 1143 mm, the strain on the web surface under vertical force is about 0, and the strain on the web surface under lateral force is 8.750×10^{-6}. For the outer side of the web, at a radius of 874 mm, the strain on the web surface under lateral force is about 0, and under vertical force, the strain on the web surface is 3.977×10^{-6}. At the location with a radius of 1024 mm, the strain on the web surface under lateral force is about 0, and the strain on the web surface under vertical force is -3.632×10^{-6}. At a radius of 944 mm, the strain on the web surface under vertical force is about 0, and the strain on the web surface under lateral force is 5.166×10^{-6}. In summary, the inner radius 870 mm of the web is selected as the strain gauge mounting location for measuring vertical force, and the inner radius 1143 mm of the web is selected as the strain gauge mounting location for measuring lateral force.

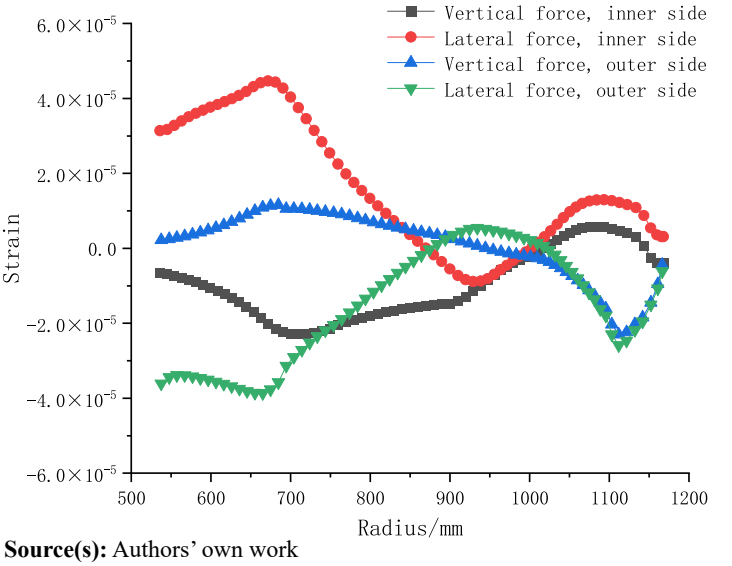

Figure 8.
Strains on the web surface with different wheel-rail forces

Source(s): Authors' own work

6. Conclusions

(1) Due to the track wheel web's unique curved shape and wheel-rail force loading mechanism, both tensile and compressive states exit on the surface of the web. Under the action of vertical force, Mises stress and strain near the inner radius of 710 mm and the outer radius of 1110 mm of the web are relatively higher, both occurring at the curve position and in a compressed state. Under lateral force, higher Mises stress and strain are observed near the radius of 670 mm on the inner and outer sides of the web, both occurring at the curve position near the root of the web. The inner surface experiences tension, while the outer surface is under compression.

(2) Under the action of vertical force, as the position of the wheel-rail force application point shifts laterally toward the outer side, the Mises stress and strain gradually decrease near the inner radius of 710 mm of the web, whereas the Mises stress and strain gradually increase near the outer radius of 1110 mm of the web. Under lateral force, the Mises stress and strain on the surface of the web remain relatively stable regardless of the position of the wheel-rail force application point.

(3) Based on the analysis of stress and strain on the surface of the web under different wheel-rail forces, the inner radius of 870 mm is recommended as the optimal strain gauge mounting location for measuring vertical force, and the inner radius of 1143 mm is suitable for measuring the lateral force. The minimal coupling interference between vertical and lateral forces at these locations offers valuable guidance for the design of track wheel force measurement systems.

References

Bižić, M., Petrović, D., Tomić, M., & Djinović, Z. (2017). Development of method for experimental determination of wheel-rail contact forces and contact point position by using instrumented wheelset. *Measurement Science and Technology*, *28*(7), 075902. doi: 10.1088/1361-6501/aa666f.

Bracciali, A., Cavaliere, F., & Macherelli, M. (2014). Review of instrumented wheelset technology and applications. In *Proceedings of the Second International Conference on Railway Technology: Research, Development and Maintenance*, Ajaccio, Corsica, France (p. 167).

Cai, C., He, Z., Tao, T., Deng, D., Zhang, S., & Shen, K. (2023). Electrical bridge scheme of urban rail transit vehicle curved radial plate force-measuring wheelset based on continuous measurement method. *Urban Mass Transit*, *26*(10), 55–60, (in Chinese).

Cazzulani, G., Gialleonardo, E., Bionda, S., Bassetti, M., Crosio, P., & Braghin, F. (2017). A new approach for the evaluation and the improvement of the metrological characteristics of an instrumented wheelset for the measure of wheel-rail contact forces. In *Proceedings of the Institution of Mechanical Engineers, Part F: Journal of Rail and Rapid Transit*, *231*(4), 381–393. doi: 10.1177/0954409716631785.

Chang, C., Wang, C., Li, L., & Zeng, Y. (2007). Study on numerical test of instrumented wheelset for continuous measurement. *Railway Locomotive & Car*, *27*(5), 3–5+54, (in Chinese).

Chu, G., Li, G., & Zu, H. (2011). Finite element analysis on the instrumented wheelset of high speed EMU. *Railway Locomotive & Car*, *31*(1), 90–93, (in Chinese).

Guo, H. (2020). *Research on online continuous measurement method of straight spoke instrumented wheelset*. Chengdu: Southwest Jiaotong University. (in Chinese).

Hao, H. (2023). *Research on the scheme of wheel rail force instrumented wheelset bridge scheme in urban rail transit*. Shijiazhuang: Shijiazhuang Tiedao University. (in Chinese).

Hou, W., Wang, W., & Zeng, Y. (2010). Research on high-precision, high-speed and continuously measured dynamic wheel-rail forces. *Journal of the China Railway Society*, *32*(1), 24–29, (in Chinese).

Hu, A., Zu, H., Zhang, Z., Chu, G., & Zhang, L. (2012). Development of a new calibration table of instrumented wheelset. *Railway Locomotive & Car*, *32*(1), 62–66, (in Chinese).

Li, J. (2015). *Development of instrumented wheelset calibration table and research on calibration technology*. Beijing: Beijing Jiaotong University. (in Chinese).

Otter, D., El-Sibaie, M., & Higgins, R. (1991). A design for next generation load measuring wheel sets. In *Proceedings of the 1991 IEEE/ASME Joint Railroad Conference*, St. Louis, MO, USA (pp. 37–42).

Ren, Y. (2012). *Research on key technology of wheel/rail contact status measurement*. Chengdu: Southwest Jiaotong University. (in Chinese).

Ren, Y., & Chen, J. (2019). A new method for wheel-rail contact force continuous measurement using instrumented wheelset. *Vehicle System Dynamics*, *57*(2), 269–285. doi: 10.1080/00423114.2018.1460853.

Zeng, Y., Wang, W., Gan, D., Zhou, D., Wang, C., He, Q., . . . Huang, Q. (1998). Theory of high accuracy load measuring wheelset. *Journal of the China Railway Society*, *20*(6), 28–34, (in Chinese).

Zhang, Y. (2016). *Design of a calibration test bench for instrumented wheelset and research of the key technology*. Chengdu: Southwest Jiaotong University. (in Chinese).

Zhong, X., Kou, J., Zhang, J., & Wang, C. (2020). Simulation and experimental study on continuous force-measuring wheelset of metro vehicles. *Machinery Design & Manufacture*, 10, 295–298, (in Chinese).

Zhu, M. (2015). *Research on straight plate instrument wheelset method*. Chengdu: Southwest Jiaotong University. (in Chinese).

Corresponding author
Yuanwu Cai can be contacted at: yuanwucai@163.com